Effect of earthquake ground motions on fragility curves of highway bridge piers based on numerical simulation

Kazi R. Karim*,† and Fumio Yamazaki

Institute of Industrial Science, University of Tokyo, Tokyo 153-8505, Japan

SUMMARY

Fragility curves express the probability of structural damage due to earthquakes as a function of ground motion indices, e.g., PGA, PGV. Based on the actual damage data of highway bridges from the 1995 Hyogoken-Nanbu (Kobe) earthquake, a set of empirical fragility curves was constructed. However, the type of structure, structural performance (static and dynamic) and variation of input ground motion were not considered to construct the empirical fragility curves. In this study, an analytical approach was adopted to construct fragility curves for highway bridge piers of specific bridges. A typical bridge structure was considered and its piers were designed according to the seismic design codes in Japan. Using the strong motion records from Japan and the United States, non-linear dynamic response analyses were performed, and the damage indices for the bridge piers were obtained. Using the damage indices and ground motion indices, fragility curves for the bridge piers were constructed assuming a lognormal distribution. The analytical fragility curves were compared with the empirical ones. The proposed approach may be used in constructing the fragility curves for highway bridge structures. Copyright © 2001 John Wiley & Sons, Ltd.

INTRODUCTION

The actual damages [1, 2] to highway systems from recent earthquakes have emphasized the need for risk assessment of the existing highway transportation systems. The vulnerability assessment of bridges is useful for seismic retrofitting decisions, disaster response planning, estimation of direct monetary loss, and evaluation of loss of functionality of highway systems. Hence, it is important to know the degree of damages [1, 3, 4] of the highway bridge structures due to earthquakes. To estimate a damage level (slight, moderate, extensive, and complete) of highway bridge structures, fragility curves [1–3, 5] are found to be a useful tool. Fragility

---

* Correspondence to: Kazi R. Karim, Yamazaki Laboratory, Institute of Industrial Science, University of Tokyo, 4-6-1 Komaba, Meguro-ku, Tokyo 153-8505, Japan.
† E-mail: kazi@rattle.iis.u-tokyo.ac.jp

curves show the relationship between the probability of highway structure damages and the ground motion indices. They allow estimating a damage level for a known ground motion index.

The 1995 Hyogoken-Nanbu (Kobe) earthquake, which is considered as one of the most damaging earthquakes in Japan, caused severe damages to expressway structures in Kobe area. Based on the actual damage data from the earthquake, a set of empirical fragility curves [1] was constructed. The empirical fragility curves give a general idea about the relationship between the damage levels of the highway structures and the ground motion indices. These fragility curves may be used for damage estimation of highway bridge structures in Japan. However, the empirical fragility curves do not specify the type of structure, structural performance (static and dynamic) and variation of input ground motion, and may not be applicable for estimating the level of damage probability for specific bridge structures [5].

The objective of this study is to develop analytical fragility curves based on numerical simulation considering both structural parameters and variation of input ground motion. It is assumed that structural parameters and input motion characteristics (e.g., frequency contents, phase, and duration) have influence on the damage to the structure for which there will be an effect on the fragility curves. In this study, we consider a RC bridge structure. The piers of the bridge structure are designed [6, 7] using the seismic design codes [8] for highway bridges in Japan. Using the strong motion records from Japan and the United States, the damage indices [9] of the bridge piers are obtained from a non-linear dynamic response analysis [10]. Then, using the obtained damage indices and the ground motion indices, the fragility curves for the bridge piers are constructed. The fragility curves developed by following this approach are compared with the empirical ones [1]. The proposed approach may be used in constructing fragility curves for the bridge piers, which do not have enough earthquake experience.

DEVELOPMENT OF FRAGILITY CURVES

Empirical fragility curves

Yamazaki *et al.* [1] developed a set of empirical fragility curves based on the actual damage data from the 1995 Hyogoken-Nanbu earthquake and showed the relationship between the damages occurred to the expressway bridge structures and the ground motion indices. In the empirical approach, a total of 216 bridge structures of the Japan Highway Public Corporation (JH) were taken into account among which around 50 per cent of the bridges were constructed during the period using the 1964 seismic design code. The damage data of the JH expressway structures due to the Hyogoken-Nanbu earthquake were collected, and the ground motion indices along the expressways were estimated based on the estimated strong motion distribution using the Kriging technique. The damage data and ground motion indices were related to each damage rank [1, 3, 4]. Using a certain range of ground motion indices, the damage ratio was obtained. Finally, using the results of the damage ratio for each damage rank, the empirical fragility curves for the expressway bridge structures were constructed assuming a lognormal distribution [1, 11]. The empirical fragility curves obtained following this approach do not consider structural parameters and variation of input ground motion due to the shortage of data. Hence, these curves may not be applicable to the class of structures, which were not considered in developing them. It is noted that if we specify a bridge, its fragility curves have small variability, only including randomness due to the variation of input motion.
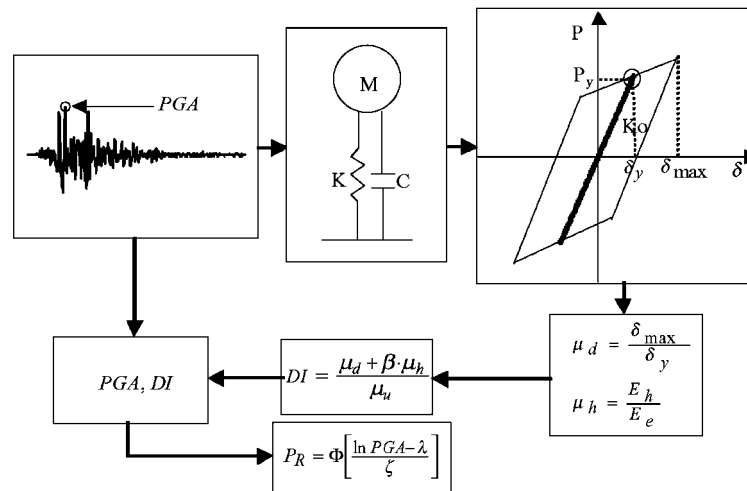
Figure 1. Schematic diagram for constructing the fragility curves for RC bridge piers.

Analytical fragility curves

In this study, we consider an analytical approach to construct the fragility curves for bridge piers of specific bridges. The piers are designed using the 1964 and 1998 seismic design codes [8] for highway bridges in Japan. The yield stiffness of the piers is obtained performing the sectional and static analysis [12]. A non-linear dynamic response analysis of the piers is performed using this yield stiffness. For the non-linear dynamic response analysis, the piers are modelled as a single-degree-of-freedom (SDOF) system [10, 13].

For a non-linear dynamic response analysis and to get a wider range of the variation of input ground motion, strong motion records were selected from the 1995 Hyogoken-Nanbu ($M_W = 6.9$, $M_{JMA} = 7.2$), the 1994 Northridge ($M_W = 6.7$), the 1993 Kushiro-Oki ($M_{JMA} = 7.8$) and the 1987 Chibaken-Toho-Oki ($M_{JMA} = 6.7$) earthquakes. A total of 50 acceleration time histories were taken from each earthquake event. The acceleration time histories were chosen on the basis of large peak ground acceleration (PGA) values (at least larger than 100 cm/s^2 for a larger horizontal component). Both the EW and NS components are employed to generate a large number of records.

Using these acceleration time histories as an input motion, the damage indices [9] of the bridge piers are obtained from the non-linear analysis [10]. Finally, using the obtained damage indices and the ground motion indices, the analytical fragility curves for RC bridge piers are constructed. The fragility curves obtained by this approach consider both structural parameters and variation of input ground motion. The schematic diagram for constructing the analytical fragility curves is shown in Figure 1. The steps for constructing the analytical fragility curves are as follows:

1. Select the earthquake ground motion records.
2. Normalize PGA of the selected records to different excitation levels.
3. Make an analytical model of the structure.

Earthquake Engng Struct. Dyn. 2001; **30**:1839–1856

4. Obtain the stiffness of the structure.
5. Select a hysteretic model for the non-linear dynamic response analysis.
6. Perform the non-linear dynamic response analysis using the selected records.
7. Obtain the ductility factors of the structure.
8. Obtain the damage indices of the structure in each excitation level.
9. Calibrate the damage indices for each damage rank.
10. Obtain the number of occurrences of each damage rank in each excitation level and get the damage ratio.
11. Construct the fragility curves using the obtained damage ratio and the ground motion indices for each damage rank.

STATIC ANALYSIS

A typical bridge structure is considered. The bridge model taken in this study is rather simple. The length of each span of the bridge is 40 m and the width is 10 m. The height of each pier is 8.5 m. The cross-section of each pier is $4 \text{ m} \times 1.5 \text{ m}$. The total weight is 5163 kN, calculated as the weight of the superstructure (deck and girder) and weight of the substructure (pier). The weight of the superstructure is 4416 kN and self-weight of the pier is 1494 kN. The piers are designed by using the 1964 and 1998 seismic design codes [8] in Japan and are named as the 1964 pier and the 1998 pier. The fundamental period for the two piers is 0.30 s and 0.27 s, respectively. Figure 2(a) shows the elevation of a typical bridge pier.

Sectional analysis

The sectional analysis is carried out for two reasons: (1) to find out the two possible failure modes, i.e., shear or flexural failure modes of the bridge piers and (2) to obtain the force–displacement relationship at the top of the bridge piers. The moment–curvature and shear vs shear strain relationships of the cross-sections are obtained using the programme RESPONSE-2000 [12]. The analytical procedures in RESPONSE-2000 are based on the traditional engineering beam theory, which assumes that plane sections remain plane and that the distribution of shear stresses across the section is defined by the rate of change of flexural stresses. For sectional analysis, yield strength of steel (σ_{sy}) and compressive strength of concrete (σ_c') are taken as 332 and 27 MPa, respectively. The longitudinal (area ratio) and tie reinforcement (volumetric ratio) for the 1964 pier are taken as 1.21 and 0.09 per cent, respectively, and they are taken as 1.36 and 1.03 per cent, respectively for the 1998 pier.

   Figures 2(b), 2(c) and 2(d) show the sectional views and properties of concrete and reinforcement bar, which are used in the RESPONSE-2000 program. It should be noted that for simplicity and analysis purpose, single arrangement of the main reinforcement bars has been used instead of the double arrangement. However, one can see that there is significant change of the provision and configuration of the tie reinforcement from 1964 to 1998 code specifications. Figure 4(a) shows the shear vs shear strain relationship for the cross-section at the base level of the 1964 pier and the moment–curvature relationship for the cross-section at the base level of the 1998 pier is shown in Figure 4(b). From the sectional analysis, it is found that the shear failure governs the failure mode in the case of the 1964 pier and the flexural failure governs the failure mode in the case of the 1998 pier. Note that after the

(a) Elevation of a typical bridge pier

(b) Cross-section (c-c) of 1964 pier   (c) Cross-section (c-c) of 1998 pier
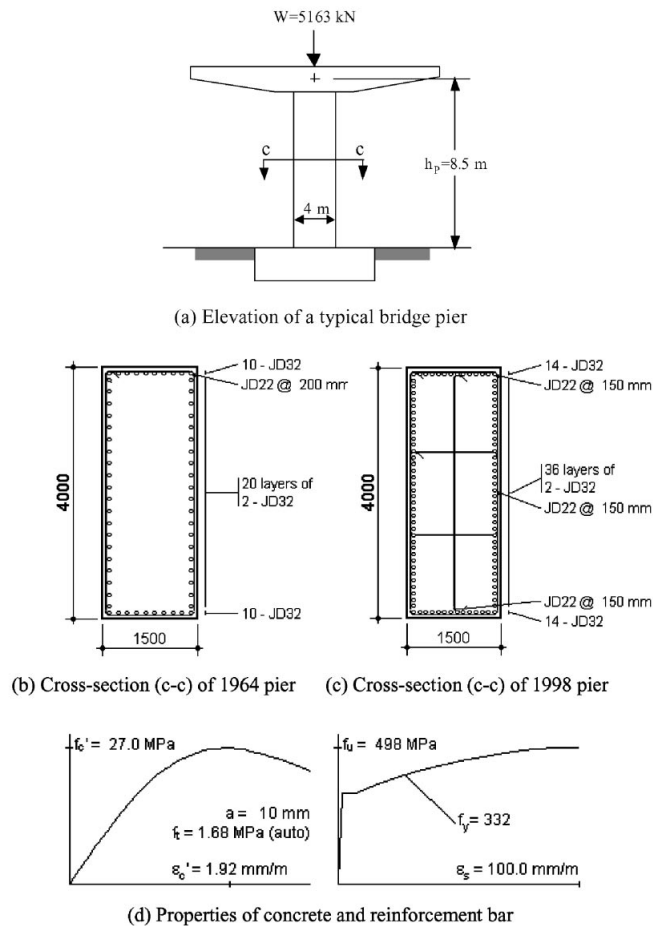
(d) Properties of concrete and reinforcement bar

Figure 2. Elevation, sectional view, and properties of concrete and reinforcement
bar of the bridge piers used in this study.

Kobe earthquake, Kawashima *et al.* [14] evaluated the performance of the Japanese bridge piers designed with different seismic design codes, and concluded that bridge piers designed before 1980 fail mostly in shear and bridge piers designed after 1980 fail mostly in flexure.

Static pushover analysis

To obtain the force–displacement relationship at the top of the bridge pier, the pier is divided into N slices (50 slices are recommended in the code) along its height [8]. It should be noted that as the 1964 pier fails in shear, the shear analysis is carried out for the cross-sections of the 1964 pier and as the 1998 pier fails in flexure, the flexural analysis is carried out for the cross-sections of the 1998 pier. For sectional analysis, it is mainly focused on three sections: (1) section at the top level, (2) section at the one-third level from the bottom of the pier,
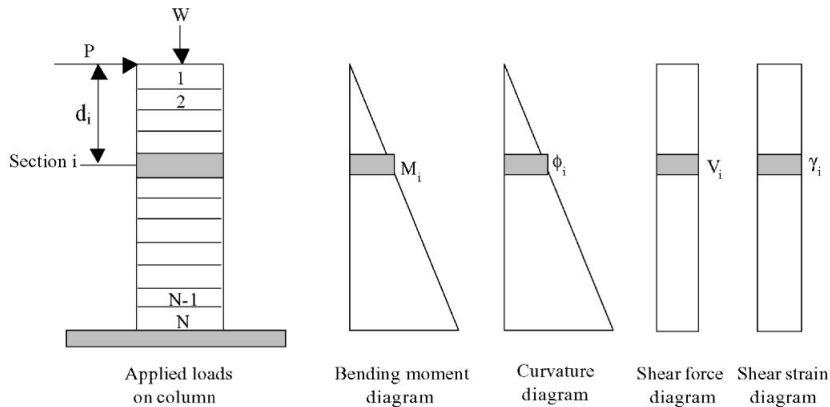
Figure 3. Numerical evaluation of flexural and shear components of displacement.

and (3) section at the base level. This is because the configuration of the reinforcement at these levels is different. Finally, the force–displacement relationship at the top of the bridge pier is obtained using the shear vs shear strain and moment–curvature diagrams. Figure 3 shows the numerical evaluation of the flexural and shear components of the displacement. In case of flexural analysis, there is no contribution of the shear component to the displacement, however, in the case of shear analysis, there is contribution of both the shear and flexural components to the displacement. The steps for obtaining the force–displacement curve are as follows:

1. Divide the pier into N slices along its height.
2. Obtain the shear vs shear strain (from shear analysis) and moment–curvature (from flexural analysis) diagrams for each cross-section.
3. Apply the horizontal force P at the top of the bridge pier.
4. Obtain the shear force and bending-moment diagrams of the pier for the applied force P.
5. Get the shear strain by interpolation for each cross-section from the shear force and shear vs shear strain diagram, and curvature from bending moment and moment–curvature diagram.
6. Calculate the displacement δ using the following equation:

$$\delta = \sum_{i=1}^{N} (\phi_i \times dy \times d_i + \gamma_i \times dy) \qquad (1)$$

where δ is the displacement, N is the number of cross-sections, ϕ_i is the curvature, dy is the width of each cross-section, d_i is the distance from the top of the pier to the centre of gravity (c.g.) of each cross-section and, γ_i is the shear strain.
7. In a similar way, apply several forces P and obtain the corresponding displacements δ. Finally, using these values, obtain the force–displacement relationship at the top of the bridge pier.

Figure 4(c) shows the plots of the force–displacement relationship at the top of the bridge piers. One can see that the 1998 pier performs well compared to the 1964 pier. This might be due to the provision of the longitudinal and tie reinforcement and also due to the con-

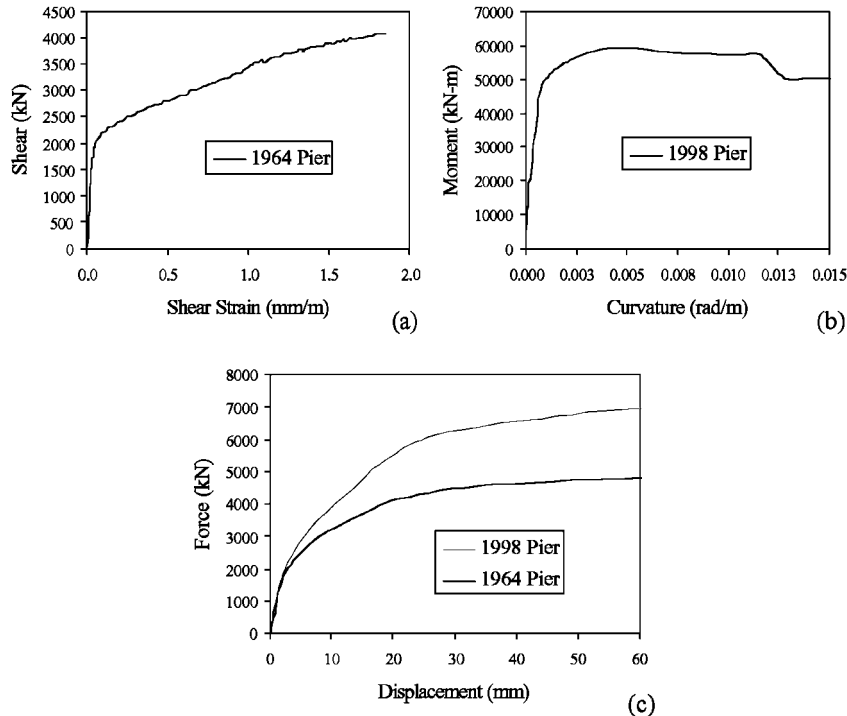*Earthquake Engng Struct. Dyn.* 2001; **30**:1839–1856

Figure 4. (a) Shear vs shear strain relationship for the cross-section at the base level of the 1964 pier, (b) moment–curvature relationship for the cross-section at the base level of the 1998 pier, and (c) force–displacement relationship at the top of the bridge piers.

figuration of the tie reinforcement. The yield force and yield displacement at the top of the pier is obtained from a bilinear assumption [7]. Yield force and yield displacement for the 1964 pier and the 1998 pier are obtained as 3920.53 kN, 1.78 cm and 5381.48 kN, 1.91 cm, respectively. The yield stiffness (K_0) of the bridge piers is obtained using the yield force and yield displacement and this value is used to perform the non-linear dynamic response analysis.

DYNAMIC ANALYSIS

The piers are modeled as a SDOF system for performing the non-linear dynamic response analysis [10]. A bilinear hysteretic model [7, 13] was considered. The post-yield stiffness was taken as 10 per cent of the secant stiffness [13] of the pier with 5 per cent damping ratio. The yield stiffness of the piers is taken from the static analysis. The ductility factor μ at the top of the bridge pier is obtained from non-linear dynamic response analysis. The total ductility demand is calculated considering both displacement and hysteretic energy ductility. The hysteretic energy ductility is considered as it contributes a significant damage to the structure. The displacement ductility μ_d is defined as the ratio of the maximum displacement (obtained from dynamic analysis) to the displacement at the yield point (obtained from static

analysis). In a similar way, the hysteretic energy ductility μ_h is defined as the ratio of the hysteretic energy to the energy at the yield point. The ductility factors thus obtained are used to evaluate the damage of the bridge piers.

Structural damage and input motion parameters

To construct a relationship between earthquake ground motion and structural damage, a data set comprising inputs (strong motion parameters) and outputs (damage) is necessary. There are two methods for doing this: (1) collect the actual earthquake records and damage data and (2) perform earthquake response analyses for given inputs and models and obtain the resultant damage (outputs). The former is more convincing because it uses actual damage data. However, earthquake records obtained near structural damage are few. With the latter, it is easier to prepare well-distributed data. Since it is not based on actual observations, however, much care should be taken in selecting structure models and input motions. The former was used by Yamazaki *et al.* and reported elsewhere [1]. The latter is used in this study.

Selection of input motion parameters to correlate with the structural damage is important, however, it is not an easy task. The PGA is a commonly used index to describe the severity of the earthquake ground motion. However, it is well known that a large PGA is not always followed by severe structural damage. Other indices of earthquake ground motion, e.g., peak ground velocity (PGV), peak ground displacement (PGD), time duration of strong motion (T_d) [15], spectrum intensity (SI) [16], and spectral characteristics, can be considered in damage estimation [17]. In this study, PGA and PGV are considered as the amplitude parameters used for fragility curves.

Even having the same PGA and PGV, it is assumed that structural damage due to different records from different earthquakes might be different. This is due to the characteristics (frequency contents, phase, duration, etc.) of the input ground motion. Figure 5 shows the histograms of the time duration [15] of the recorded accelerograms used in this study. It can be seen that maximum occurrence of T_d for the Kobe and Northridge earthquakes is around 10 s, and for the Kushiro-Oki and Chibaken-Toho-Oki earthquakes it is around 25 s. Although the source-to-site distance of each record varies, the short durations for the Kobe and Northridge events reflect their moderate magnitude and (mostly) near-source records. The long duration for the Kushiro-Oki earthquake reflects the large magnitudes and long source-to-site distance. For the Chibaken-Toho-Oki earthquake, the long duration indicates that the records are mostly far field ones.

Figure 6 shows the plots of the acceleration response spectra (normalized to $1g$) with 5 per cent damping ratio of the recorded ground motion used in this study. The mean amplitude for 50 records of each earthquake event is shown in the same figure with a thick line. Within each event, a large variation of spectral shape is seen due to mostly the soil condition and source-to-site distance. In the same figure, even normalized to $1g$, one can see that the mean spectral shapes for the Kobe, Northridge, Kushiro-Oki and Chibaken-Toho-Oki earthquakes are different. However, since the average response spectrum for each earthquake contains various different response spectra, clear explanation about its shape is difficult. Due to the variation of response amplitudes, any structure having any fundamental period T, the damage to the structure due to the four earthquake events might be different. Obviously, if we specify the structure and input motion in terms of time history, the damage to the structure due to the input motion can be obtained easily and this is a deterministic approach. However, if we
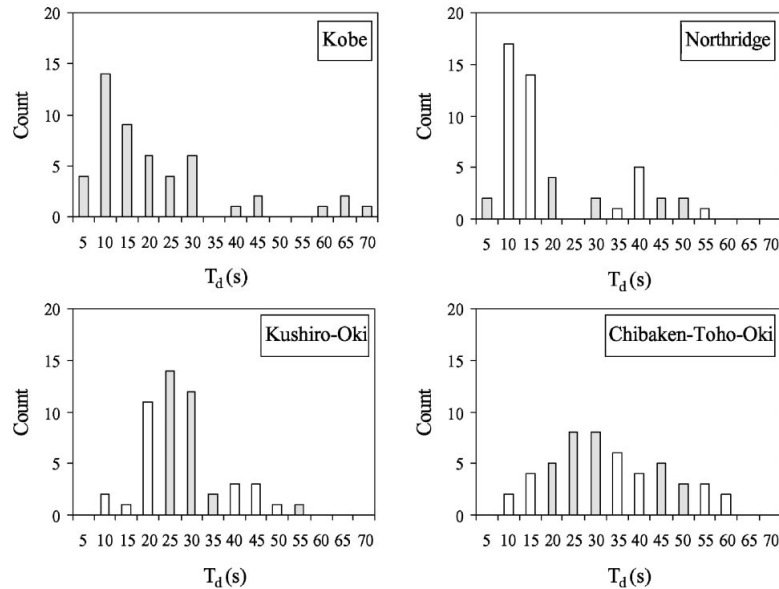
Figure 5. Histograms of the time duration (T_d) of the recorded accelerograms for different earthquake events used in this study.

want to predict damage due to future earthquakes, a probabilistic approach is necessary since we cannot specify a deterministic input motion.

Damage analysis

For the damage assessment of the bridge piers, Park–Ang [9] damage index was used in this study. The damage index DI is expressed as

$$DI = \frac{\mu_d + \beta\mu_h}{\mu_u} \tag{2}$$

where μ_d and μ_u are the displacement and ultimate ductility of the bridge piers, β is the cyclic loading factor taken as 0.15 and μ_h is the cumulative energy ductility. The ultimate ductility μ_u is defined as the ratio of maximum displacement (obtained from the static analysis) to the yield displacement (obtained from the static analysis). The cumulative energy ductility μ_h is defined as the ratio of the hysteretic energy (obtained from the dynamic analysis) to the energy at yield point (obtained from the static analysis). The value for μ_u for the 1964 pier and the 1998 pier was calculated (from static analysis) as 5.06 and 6.01, respectively. Finally, the damage indices of the bridge piers are obtained using the relationship given in Equation (2).

The obtained damage indices for the selected input ground motion are calibrated to get the relationship between the DI and damage rank (DR). This calibration is done using the method proposed by Ghobarah *et al.* [4]. Table I shows the relationship between DI and DR. It can be seen that each DR has a certain range of DI. The DR ranges from slight to complete.

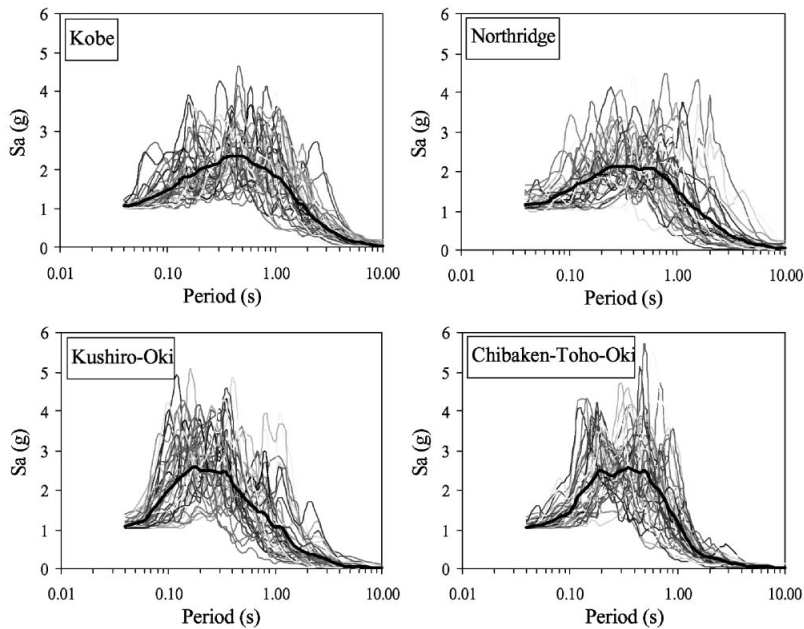*Earthquake Engng Struct. Dyn.* 2001; **30**:1839–1856

Figure 6. Acceleration response spectra (normalized to $1g$) with 5 per cent damping ratio of the recorded ground motion for different earthquake events used in this study. The mean amplitude for 50 records of each earthquake event is shown with a thick line.

Table I. Relationship between the damage index (DI) and damage rank (DR) [4].

Damage index (DI)	Damage rank (DR)	Definition
$0.00 < \mathrm{DI} \leqslant 0.14$	D	No damage
$0.14 < \mathrm{DI} \leqslant 0.40$	C	Slight damage
$0.40 < \mathrm{DI} \leqslant 0.60$	B	Moderate damage
$0.60 < \mathrm{DI} < 1.00$	A	Extensive damage
$1.00 \leqslant \mathrm{DI}$	As	Complete damage

Using the relationship between DI and DR, the number of occurrence of each damage rank is obtained. These numbers are then used to obtain the damage ratio for each damage rank.

To count the number of occurrence of each damage rank, PGA for the selected records were normalized to different excitation levels. The upper limit for the excitation level was restricted in such a way that its value should be close to the maximum PGA value of the selected records for each earthquake event. For instance, the maximum PGA for the records of the Kobe earthquake was $818.01 \, \mathrm{cm/s^2}$. Hence, PGA for the records of the Kobe earthquake were normalized from 100 to 1000 $\mathrm{cm/s^2}$ having 10 excitation levels with equal intervals. Then, the ground motion records are applied to the structure to obtain the damage indices. Using these damage indices, the number of occurrence of each damage rank is obtained for each excitation level. Finally, using the numbers the damage ratio is obtained for each damage rank.

In case of PGV, the number of occurrence of each damage rank is counted following almost the same method that is applied for PGA but in a slightly different way. For a single earthquake event, the same method (as in the case of PGA) can be applied [18]. However, for different earthquake events, as the level of PGV after scaling is quite different from the actual one, application of the same method may give very unrealistic results. Hence, in this study, the scaling used for PGA was also applied to PGV to scale it up (or scale down) for each record. The obtained PGV values were then arranged with 10 excitation levels having some suitable intervals. Finally, the number of occurrence of each damage rank is obtained in each excitation level and the damage ratio is obtained using the numbers.

Numerical examples

To demonstrate how the DI, DR, number of occurrence of each damage rank, and the damage ratio are obtained, first consider the 1964 pier and the 1995 Kobe earthquake. As it was mentioned earlier that 50 records were selected from this earthquake. Each record has different PGA and PGV. Now, normalize the PGA of each record to $1000 \, \text{cm/s}^2$ and apply it to the structure (1964 pier). After performing the dynamic response analysis, the damage indices are obtained using Equation (2). For example, the damage index obtained for the JMA Kobe-NS record is 0.96. Calibrating this DI using Table I, one can see that the corresponding DR is 'extensive'. Similarly, the DI for the other records at the ground excitation level $1000 \, \text{cm/s}^2$ is calibrated to obtain the corresponding damage rank. The number of occurrence of each damage rank (no, slight, moderate, extensive, and complete) at this ground excitation level is counted as 0, 3, 2, 5 and 40. The damage ratio is obtained using these numbers. The damage ratio is defined as the number of occurrence of each damage rank divided by the total number of records. For example, the damage ratio for the complete damage case (at ground excitation level $1000 \, \text{cm/s}^2$) is 0.8, which comes out as dividing 40 (number of occurrence) by 50 (total number of records). Same procedure has also been applied for the other ground excitation levels. Finally, the damage ratios are fitted by the least-squares method on a lognormal probability paper, which is used to obtain the fragility curves.

Figure 7 shows the plots of the responses for the bridge piers due to the different earthquake events. The corresponding damage indices and damage ranks are also shown in the figure. It can be seen that (Figure 7(a)) for the same record (JMA Kobe-NS), the DI obtained for the 1964 pier (DI = 0.96) is higher compared to the one obtained for the 1998 pier (DI = 0.43). The corresponding DR obtained for the two piers are 'extensive' and 'slight', respectively. It means, changing the structural parameters influences the damages to the structure. It can also be seen that (Figure 7(b)) even having the same excitation level, the DI obtained for the different input motions are different and the corresponding DR is also different. The DI obtained for the JMA Kobe-NS, Sylmar-360, JMA Kushiro-EW, and Mobara-EW are 0.96, 1.37, 0.62 and 0.42, respectively and the corresponding DR are 'extensive', 'complete', 'extensive', and 'moderate', respectively. This implies that the characteristics of strong motion records (frequency contents, duration, phase, etc.) have influence on the occurrence of damage to the structure.

Figure 8(a) shows the number of occurrence of each damage rank in different excitation levels for the 1964 pier due to the Kobe earthquake. It can be seen for PGA that as the excitation level increases the number of occurrence of slight damage decreases, whereas the number of occurrence of complete damage increases. Similar trend is also seen in the plot
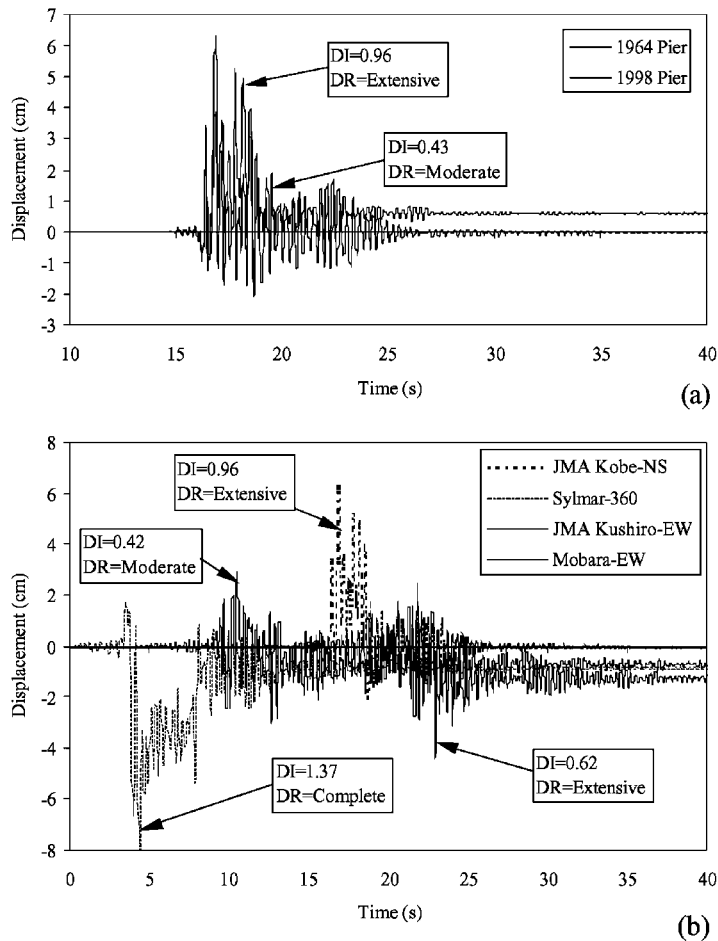
Figure 7. Comparison of the responses for (a) the 1964 and the 1998 piers due to the JMA Kobe-NS record scaled to 1g, and (b) the 1964 pier due to the different input motions scaled to 1g. They are JMA Kobe-NS record from the 1995 Kobe EQ, Sylmar-360 record from the 1994 Northridge EQ, JMA Kushiro-EW record from the 1993 Kushiro-Oki EQ, and Mobara-EW record from the 1987 Chibaken-Toho-Oki EQ.

(Figure 8(b)) for PGV although the number of data that belongs to each excitation level is different due to the scaling scheme used.

FRAGILITY CURVES

Fragility curves are constructed with respect to both PGA and PGV. The damage ratio for each damage rank in each excitation level (with respect to both PGA and PGV) is obtained by calibrating the DI using Table I. Based on these data, fragility curves for the bridge piers
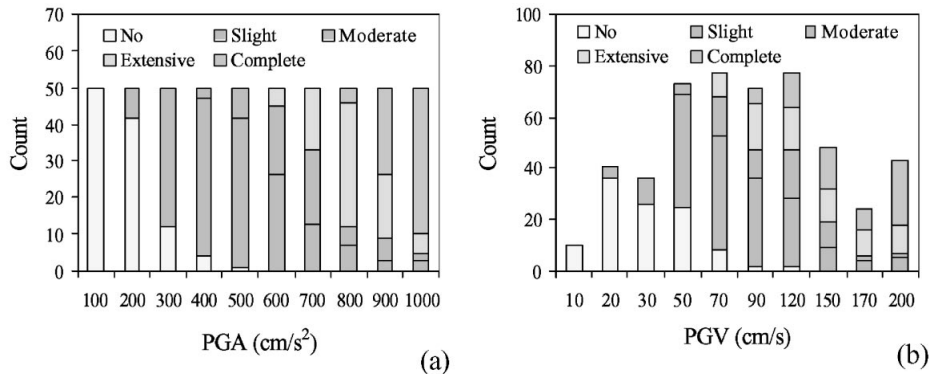
Figure 8. Number of occurrence of each damage rank in different excitation levels (a) with respect to PGA, and (b) with respect to PGV for the 1964 pier due to the Kobe earthquake. The input motion were scaled based on PGA.

Table II. Parameters of fragility curves for the studied RC bridge piers with respect to PGA.

Event and pier	Damage rank (DR)							
	DR $\geqslant$ C		DR $\geqslant$ B		DR $\geqslant$ A		DR = As	
	λ	ζ	λ	ζ	λ	ζ	λ	ζ
Kobe (empirical)	6.36	0.29	6.46	0.30	6.67	0.29	6.87	0.32
Kobe (1964 pier)	5.56	0.30	6.42	0.27	6.62	0.20	6.82	0.11
Kobe (1998 pier)	6.14	0.28	6.87	0.20	7.05	0.17	7.23	0.16
Northridge (1964 pier)	5.57	0.37	6.43	0.28	6.64	0.23	6.85	0.15
Kushiro (1964 pier)	5.31	0.48	6.20	0.53	6.50	0.50	6.81	0.46
Chibaken (1964 pier)	5.47	0.30	6.31	0.20	—	—	—	—

are constructed assuming a lognormal distribution [1, 11]. For the cumulative probability P_R of occurrence of the damage equal or higher than rank R is given as

$$P_R = \Phi \left[\frac{\ln X - \lambda}{\zeta} \right] \tag{3}$$

where Φ is the standard normal distribution, X is the ground motion indices (PGA and PGV), λ and ζ are the mean and standard deviation of $\ln X$. Two parameters of the distribution (i.e., λ and ζ) are obtained by the least-squares method on a lognormal probability paper. Using these probability papers, the two parameters of the distribution are obtained to construct the fragility curves of the bridge piers due to the four earthquake events.

The obtained values of λ and ζ for $\ln X$ are given in Tables II and III, respectively. It can be seen that no value has been entered (Table II) for the extensive and complete damage cases with respect to PGA due to the 1987 Chibaken-Toho-Oki earthquake. This is because 'extensive' and 'complete' damages were not observed due to this earthquake. Similarly, with respect to PGV, complete damage was not observed (Table III) due to this earthquake. For

Table III. Parameters of fragility curves for the studied RC bridge piers with respect to PGV.

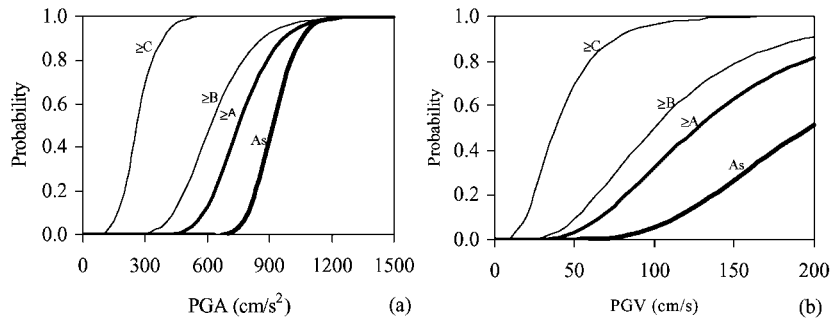| Event and pier	Damage rank (DR)							
	DR $\geqslant$ C		DR $\geqslant$ B		DR $\geqslant$ A		DR $=$ As	
	λ	ζ	λ	ζ	λ	ζ	λ	ζ
Kobe (empirical)	4.10	0.35	4.27	0.36	4.55	0.40	4.82	0.40
Kobe (1964 pier)	3.64	0.53	4.60	0.52	4.84	0.51	5.28	0.53
Kobe (1998 pier)	4.21	0.54	4.92	0.44	5.12	0.41	5.31	0.36
Northridge (1964 pier)	3.30	0.61	4.13	0.82	4.66	0.86	5.29	0.77
Kushiro (1964 pier)	2.68	0.63	3.64	0.83	4.00	0.87	4.66	0.99
Chibaken (1964 pier)	3.59	0.40	4.32	0.30	4.47	0.20	—	—

Figure 9. Fragility curves for the 1964 pier (a) with respect to both PGA, and (b) with respect to PGV obtained from the records of the Kobe earthquake.

a comparison of the empirical and analytical fragility curves, the parameters λ and ζ for the empirical fragility curves were taken from the previous study [1]. Finally, the fragility curves for damage ranks are plotted in Figure 9 with respect to both PGA and PGV obtained for the 1964 pier due to the Kobe earthquake.

Figure 10 shows the plots of the empirical and analytical fragility curves for the 1964 pier and the 1998 pier obtained from the Kobe earthquake with respect to both PGA and PGV. Note that there are five damage ranks that are shown in Table I. For simplicity, the fragility curves only for 'moderate' and 'complete' damage cases are shown in the plots. One can see that the empirical and analytical fragility curves of the 1964 bridge pier show a very similar level of damage probability with respect to PGA except the complete damage case, although the other two damage cases, i.e., 'slight' and 'extensive' are not shown in the plot. However, with respect to PGV, some difference is observed between the two. Several reasons are considered to explain this difference: (1) PGA and PGV were estimated by the Kriging technique in the empirical fragility curves, while they are obtained from the input motion of the response analysis in this study, (2) only one pier model is used in this study, while in the empirical approach, various bridge structures were considered to construct the fragility curves.

It can also be seen (Figure 10) that the analytical fragility curves of the 1964 and the 1998 piers show a very different level of damage probability with respect to both PGA and PGV.
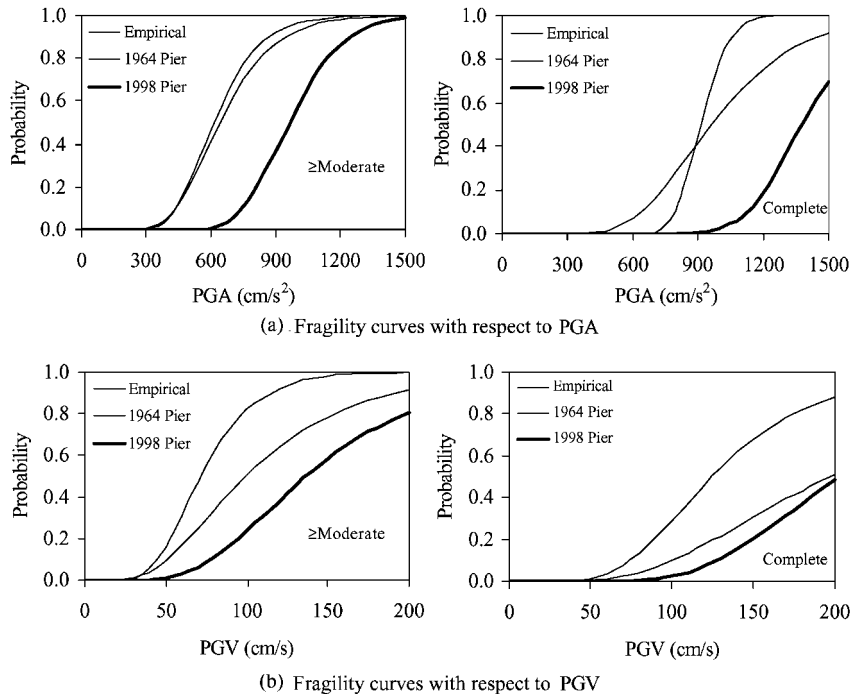
Figure 10. Comparison of the analytical fragility curves for the 1964 and 1998 piers (a) with respect to PGA, and (b) with respect to PGV obtained from the records of the Kobe earthquake. The empirical fragility curves [1] are also shown in the figure.

As the level of PGA and PGV increases, the analytical fragility curves of the 1964 pier show a higher level of damage probability compared to that of the 1998 pier. This difference is due to: (1) the provision of the longitudinal and tie reinforcement and (2) the configuration of the tie reinforcement for the two codes. The longitudinal and tie reinforcement has been changed significantly for the 1998 code compared to the 1964 one. The provision of reinforcement results in the 1998 pier performing well against the seismic action compared to the 1964 pier.

   Figure 11 shows the plots of the empirical and the analytical fragility curves for the 1964 bridge pier obtained from the Kobe, Northridge, Kushiro-Oki and Chibaken-Toho-Oki earthquakes with respect to both PGA and PGV. It can be seen that the level of damage probability due to the different earthquake events is quite different with respect to both PGA and PGV, however, it is observed that the Kobe and Northridge earthquakes show a similar level of damage probability for the 'moderate' and 'complete' damage cases with respect to PGA. One can see that in the case of moderate damage, the Chibaken-Toho-Oki earthquake shows higher level of damage probability with respect to PGA compared to the other events. The same event shows no complete damages with respect to PGA. One can also see that with respect to PGV, Chibaken-Toho-Oki earthquake shows a lower level of damage probability compared to the other events in the case of moderate damage when the PGV is around 70cm/s or less and the same event shows no complete damage with respect to PGV. The reason for this might be due to the fact that the Chibaken-Toho-Oki earthquake has small magnitude
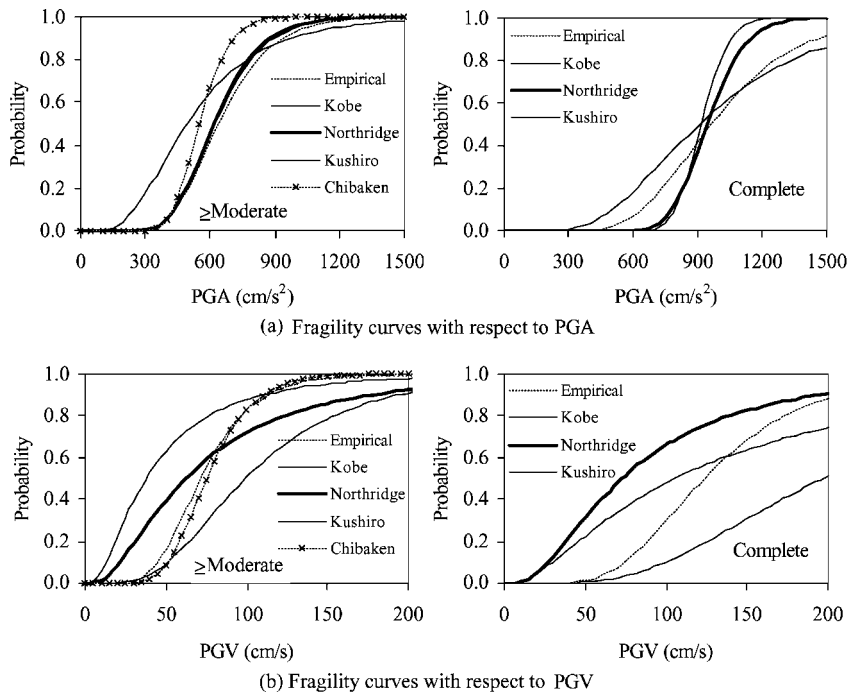
Figure 11. Comparison of the analytical fragility curves for the 1964 pier (a) with respect to PGA and, (b) with respect to PGV obtained from the records of different earthquake events. The empirical fragility curves [1] are also shown in the figure.

and hence its records are not so damaging even after scaling. One should also notice that the Kushiro-Oki earthquake shows higher level of damage probability for the lower value of both PGA and PGV and the large magnitude and long duration of this earthquake might cause higher level of damage probability. As the ground motion level increases, the Kobe and Northridge earthquakes show a higher level of damage probability than other events with respect to PGA, while with respect to PGV, the Northridge earthquake shows a higher level of damage probability than the Kobe earthquake. Since the scaling scheme is employed in this study, a more detailed discussion on the effect of input motion to structural damage is difficult. However, we could demonstrate the fact that fragility curves are dependent on the duration and spectral characteristics of earthquake ground motion as well as the excitation level.

CONCLUSIONS

A numerical method to construct fragility curves for bridge piers of a specific bridge has been presented based on static sectional and pushover analyses and dynamic non-linear analysis. The analytical fragility curves for the piers designed by the 1964 and 1998 Japanese highway bridge codes were constructed with respect to both PGA and PGV. As an input motion to the

models, the strong motion records were selected from the 1995 Kobe, the 1994 Northridge, the 1993 Kushiro-Oki, and the 1987 Chibaken-Toho-Oki earthquakes. The obtained analytical fragility curves were compared with the empirical ones developed based on the actual damage data due to the Kobe earthquake.

Similar level of damage probability was observed for the empirical and analytical fragility curves of the 1964 bridge pier with respect to PGA except for the complete damage case but some difference was observed with respect to PGV. It is not realistic to compare the empirical and analytical fragility curves as both are constructed using two different methods. Since, both the method and the input data are different, the two platforms are not compatible. However, for research purposes and to give an idea to the readers how the empirical fragility curves differ from that of the analytical one, it is included and as well as compared in this study.

The analytical fragility curves of the 1964 bridge pier showed a higher level of damage probability with respect to both PGA and PGV compared to the analytical ones of the 1998 bridge pier. The analytical fragility curves obtained by using different sets of input motion from the four earthquake events for the 1964 pier show a different level of damage probability with respect to both PGA and PGV. Thus, the fragility curves (structural damages) were found to be dependent on spectral and durational characteristics of input motion as well as the level of the amplitude. The empirical fragility curves cannot introduce various structural parameters and characteristics of input motion, and they require a large amount of actual damage data for a certain class of structures. Hence, the analytical method employed in this study may be used in constructing the fragility curves for a class of bridge structures, which do not have enough earthquake experience.

Although, only two pier models and four sets of earthquake records were used in this study, the method presented herein is useful to demonstrate the effect of structural parameters and input motion characteristics on fragility curves. However, a further study using various bridge models must be necessary to draw a solid conclusion for the fragility curves of bridge structures. Moreover, the effect of soil–structure interaction is not considered for constructing the analytical fragility curves in this study for which a further study is also necessary.

REFERENCES

1. Yamazaki F, Motomura H, Hamada T. Damage assessment of expressway networks in Japan based on seismic monitoring. *12th World Conference on Earthquake Engineering*, CD-ROM, 2000; Paper No. 0551.
2. Basoz N, Kiremidjian AS. Evaluation of bridge damage data from the Loma Prieta and Northridge, CA Earthquakes. *Report No.* 127, The John A. Blume Earthquake Engineering Center, Department of Civil Engineering, Stanford University, 1997:
3. Kircher CA, Nassar AA, Kustu O, Holmes WT. Development of building damage functions for earthquake loss estimation. *Earthquake Spectra* 1997; **13**(4):663–682.
4. Ghobarah A, Aly NM, El-Attar M. Performance level criteria and evaluation. *Proceedings of the International Workshop on Seismic Design Methodologies for the next Generation of Codes*, Balkema, Rotterdam, 1997; 207–215.
5. Mander JB, Basoz N. Seismic fragility curves theory for highway bridges. *Proceedings of the 5th U.S. Conference on Lifeline Earthquake Engineering*, TCLEE No. 16, ASCE, 1999; 31–40.
6. Naeim F, Anderson JC. Classification and evaluation of earthquake records for design. *The 1993 NEHRP Professional Fellowship Report*, Earthquake Engineering Research Institute, 1993.
7. Priestley MJN, Seible F, Calvi GM. *Seismic Design and Retrofit of Bridges*. Wiley: New York, 1996.
8. *Design Specifications of Highway Bridges*. Part V: Seismic Design, Technical Memorandum of EED, PWRI, No. 9801, 1998.
9. Park YJ, Ang AH-S. Seismic damage analysis of reinforced concrete buildings. *Journal of Structural Engineering*, ASCE 1985; **111**(4):740–757.

10. Chopra AK. *Dynamics of Structures*: *Theory and Application to Earthquake Engineering*. Prentice-Hall: Upper Saddle River, NJ, 1995.
11. Sucuoglu H, Yucemen S, Gezer A, Erberik A. Statistical evaluation of the damage potential of earthquake ground motions. *Structural Safety* 1999; **20**(4):357–378.
12. Bentz EC, Collins MP. Response-2000. *Software Program for Load-Deformation Response of Reinforced Concrete Section*, http://www.ecf.utoronto.ca/∼ bentz/inter4/inter4.shtml, 2000.
13. Kawashima K, Macrae GA. The seismic response of bilinear oscillators using Japanese earthquake records. *Journal of Research*, PWRI, Ministry of Construction, Japan, 1993; **30**:7–146.
14. Kawashima K, Sakai J, Takemura H. Evaluation of seismic performance of Japanese bridge piers designed with the previous codes. *Proceedings of the 2nd Japan–UK Workshop on Implications of Recent Earthquakes on Seismic Risk*, Technical Report TIT/EERG 98-6, 1998; 303–316.
15. Trifunac MD, Brady AG. A study of the duration of strong earthquake ground motion. *Bulletin of the Seismological Society of America* 1975; **65**:581–626.
16. Katayama T, Sato N, Saito K. SI-sensor for the identification of destructive earthquake ground motion. *Proceedings of the 9th World Conference on Earth. Engg.*, vol. 7, 1988; 667–672.
17. Molas GL, Yamazaki F. Neural networks for quick earthquake damage estimation. *Earthquake Engineering and Structural Dynamics* 1995; **24**(4):505–516.
18. Karim KR, Yamazaki F. Comparison of empirical and analytical fragility curves for RC bridge piers in Japan. *8th ASCE Specialty Conference on Probabilistic Mechanics and Structural Reliability*, ASCE, CD-ROM, 2000, Paper No. PMC2000-050.